



Society of Petroleum Engineers

SPE-185895-MS

The CHAOS-X Model and Uncertainty Values for Magnetic Directional Surveying

E. V. Herland, Teknova AS; C. C. Finlay and N. Olsen, DTU Space; I. Edvardsen, Baker Hughes;
E. Nordgård-Hansen, Teknova AS; K. M. Laundal, Teknova AS and Birkeland Centre for Space Science, University of Bergen; T. I. Waag, Teknova AS

Copyright 2017, Society of Petroleum Engineers

This paper was prepared for presentation at the SPE Bergen One Day Seminar held in Bergen, Norway, 5 April 2017.

This paper was selected for presentation by an SPE program committee following review of information contained in an abstract submitted by the author(s). Contents of the paper have not been reviewed by the Society of Petroleum Engineers and are subject to correction by the author(s). The material does not necessarily reflect any position of the Society of Petroleum Engineers, its officers, or members. Electronic reproduction, distribution, or storage of any part of this paper without the written consent of the Society of Petroleum Engineers is prohibited. Permission to reproduce in print is restricted to an abstract of not more than 300 words; illustrations may not be copied. The abstract must contain conspicuous acknowledgment of SPE copyright.

Abstract

The Earth's magnetic field provides a unique natural source of orientation information that is particularly useful for subsurface magnetic measurement-while-drilling (MWD) navigation. In order to utilize the MWD magnetic field measurements for calculating the orientation of the bottom hole assembly (BHA), an accurate geomagnetic reference model is needed for comparison. In this paper we present the CHAOS-X model, a new geomagnetic reference model that provides global vector field estimates of Earth's magnetic field, with high resolution in both space and time, for precision magnetic directional surveying applications.

The model is derived from more than one million satellite and ground-based observatory magnetic measurements and consists of modules representing internal sources (in the Earth's core and crust), magnetospheric sources, and ionospheric sources. Compared with previous reference models, the CHAOS-X model is particularly designed for better characterization of the time variations in the geomagnetic field. In this paper, we describe the model and present benchmark comparisons with magnetic observatory data to establish the uncertainty values required in models of wellbore positional errors in magnetic directional surveying applications.

The discrepancy between geomagnetic measurements and reference models are typically dominated by spatial variations caused by local geology. In applications requiring high accuracy, these variations can be taken into account by using a dedicated local model. In such cases, when the errors associated with local geology is small, our results show that the CHAOS-X reference model may yield a significant improvement compared with existing reference models. This result holds both when the model is used predictively and retrospectively. We also argue that using a model with an accurate description of the time variations improves recent magnetic surveys while drilling, since the description of the rapid time variations can be updated near real-time.

Introduction

Subsurface magnetic measurement-while-drilling (MWD) navigation is based on using the geomagnetic field for orientation. The standard directional survey tool sensors used in a bottom hole assembly (BHA) while drilling are three mutually orthogonally oriented magnetometers and accelerometers, where the magnetometers sense the geomagnetic field and the accelerometers are used to measure the gravity field. The main purpose of these measurements is to determine the orientation of the BHA, completely defined by the azimuth, inclination and toolface (Ekseth, 1998; Williamson, 2000; Jamieson, 2016). To use magnetic measurements to determine the orientation of the BHA, one requires a geomagnetic reference model that is as accurate as possible. Such reference models describe the changes of the geomagnetic field with both location and time, capturing the variations of its sources. Reduced MWD uncertainties require improved geomagnetic reference models that better describe (i) the spatial structure of the geomagnetic field and (ii) its time variations.

Existing models, for example the BGS Global Geomagnetic Model (BGGM) (BGS, 2016; Macmillan and Grindrod, 2010), which has long been the standard survey industry reference model (Jamieson, 2016), now globally characterizes spatial variations on length scales down to approx. 150 km (half wavelength of spherical harmonic degree 133), and capture slow, year-to-year, time variations.

Recently an alternative, the High Definition Geomagnetic Model (HDGM) from US National Oceanic and Atmospheric Administration (NOAA) (NOAA, 2016; Maus et al., 2012) and its successors developed by Magnetic Variation Services LLC, have emerged. Such models can in principle provide information on spatial variations down to approx. 30 km (half wavelength of spherical harmonic degree 720) by additionally incorporating marine magnetic and aeromagnetic survey data, where such data are available. Similar to BGGM, these models are also annually updated, and also track year-to-year time variations. NOAA also offers a real-time model of magnetic fields from the magnetosphere, called HDGM-RT (NOAA, 2016). In applications requiring higher accuracy, both BGGM and HDGM are often supplemented by a dedicated model of the spatial variations caused by local geology, a procedure known as In-Field referencing or IFR (Williamson et al., 1998).

The CHAOS-X model is, in contrast, designed to go beyond previous global reference models regarding issue (ii), better characterizing the time variations in the geomagnetic field. An example comparison between the CHAOS-X model and minute mean observatory data is shown in Fig 1. This illustrates how both daily (also called Solar Quiet, Sq) variations, as well as more irregular variations linked to solar disturbances, are followed by the CHAOS-X model. This is possible because of the use of sophisticated models of ionospheric and magnetospheric field variations, constrained by satellite and ground-based observatory data. Neither the BGGM or HDGM models include such rapid time variations. Regarding spatial variations, CHAOS-X provides global resolution down to approx. 235 km, and can easily be supplemented with dedicated local or global models if higher resolution is desired. In the section below, we present in detail the CHAOS-X model, many parts of which are already widely used for scientific applications (Olsen et al., 2006; Olsen et al., 2009; Olsen et al., 2010; Olsen et al., 2014; Finlay et al., 2015).

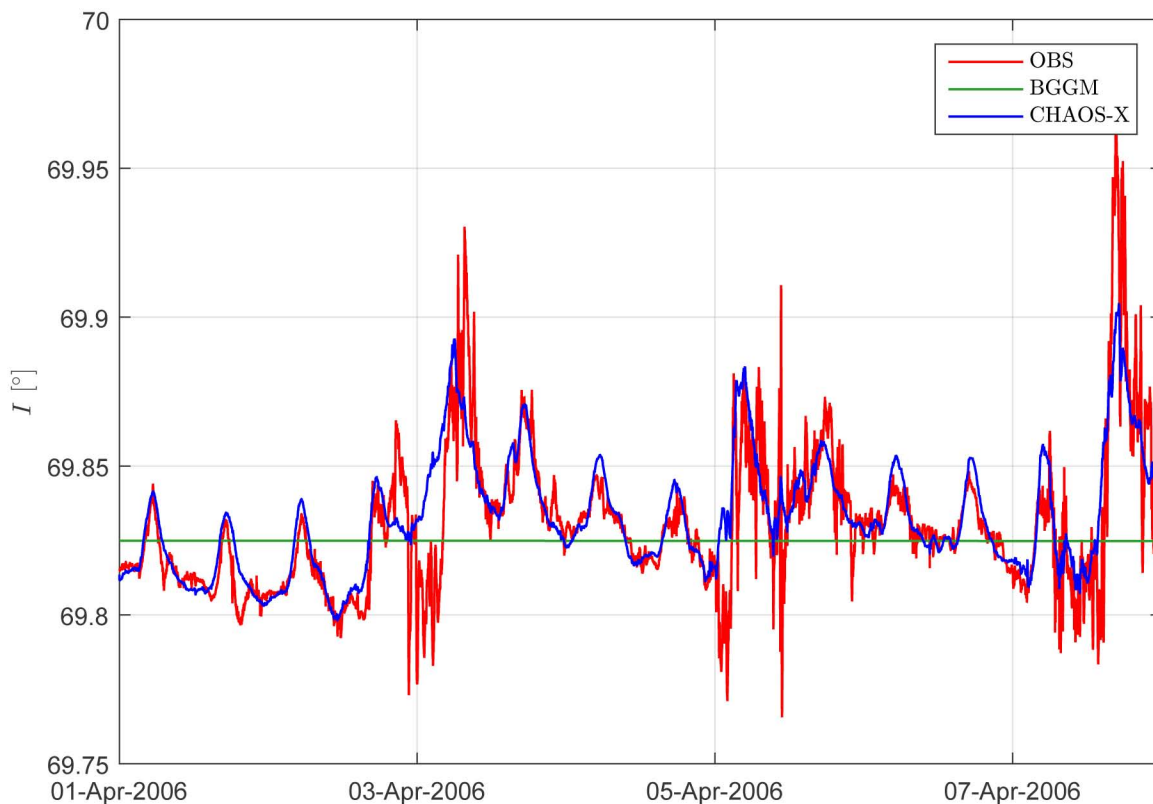


Figure 1—Example of CHAOS-X model results (blue line) compared with minute mean observatory data (red) from Brorfelde (BFE), Denmark, after removal of crustal bias. A reference model that does not account for rapid time variations (the BGGM model) is also shown for comparison (green). The figure shows results for the magnetic dip angle I . The period is 1-14 April 2006.

Of course, no reference model will perfectly capture all details of the true geomagnetic field, and thus, there will be errors associated with the model predictions. These errors translate into uncertainties in wellbore positioning, as described by the Industry Steering Committee on Wellbore Survey Accuracy (ISCWSA) error models (ISCWSA, 2016; Ekseth, 1998; Williamson, 2000; Jamieson, 2016). Specifically, there are four terms associated with the geomagnetic reference model in the ISCWSA error models: AZ, DBH, MDI and MFI. AZ is a constant contribution to the declination error while DBH is a contribution to the declination error that is dependent on the horizontal component of the geomagnetic field B_H . The total declination error is therefore given by $\sqrt{AZ^2 + (DBH/B_H)^2}$. MDI is the error in the dip angle (the angle between the magnetic field direction and horizontal direction) and MFI is the error in the magnetic field intensity. Values are typically assigned to these terms according to Table 1. In standard MWD operations, only the declination is important, and thus, only the AZ and DBH values are used. The MDI and MFI error values are included when axial interference is corrected for, and they are also used in correction algorithms and for quality control of survey data (Ekseth et al., 2006).

Table 1—Values for the geomagnetic error terms relevant for the ISCWSA error models. Values are given for BGGM, HDGM and CHAOS-X.

	AZ [°]	DBH [nT]	MDI [°]	MFI [nT]
BGGM	0.36	5000	0.20	130
HDGM	0.30	4118	0.16	107
CHAOS-X	0.36	4962	0.20	130

The values associated with using the BGGM model were originally derived by [Williamson \(2000\)](#). Subsequent improvements in magnetic data quality and distribution, as well as in geomagnetic field modelling, led Macmillan and Grindrod to propose updated uncertainty values for the BGGM model ([Macmillan and Grindrod, 2010](#)). In particular, they found that the uncertainties do not follow a simple Gaussian distribution and depend strongly on the geomagnetic latitude; they therefore published tables in which the uncertainty values could be looked up for given location (geographic latitude and longitude) and the confidence level of interest.

Uncertainty values associated with using the HDGM model were derived by [Maus et al. \(2012\)](#) by comparing predictions from the BGGM and HDGM models with magnetic measurements from a set of independent marine and airborne surveys. The BGGM model yielded an average error of 136 nT compared to an average error of 112 nT for the HDGM model. The values for the HDGM model, reproduced in [Table 1](#), were derived by scaling the BGGM values with the factor $112\text{nT}/136\text{nT} = 0.82$. In the Results section, we calculate uncertainty values for the CHAOS-X model as required for MWD navigation applications.

The CHAOS-X Reference Model

The CHAOS-X model is derived primarily from magnetic field measurements made by the low Earth orbit satellites, Ørsted, CHAMP, SAC-C and Swarm. These are supplemented by monthly mean observatory data that provide additional constraints on the slow evolution of the internal field.

The model itself consists primarily of spherical harmonic expansion coefficients that determine the magnetic field vector in an *Earth-Centered Earth-Fixed (ECEF)* coordinate system. It also includes sets of Euler angles required during the alignment of the satellite vector readings. It is the co-estimation of these Euler angles, and of external (magnetospheric) field contributions, during the model estimation procedure that enables CHAOS-X to make the optimal use of the satellite data ([Olsen et al., 2006](#)). The magnetic field vector in the ECEF frame, $\mathbf{B} = -\nabla V$, is derived from a magnetic scalar potential $V = V^{\text{int}} + V^{\text{ext}}$ consisting of a part, V^{int} , describing internal (core and lithospheric) sources, and a part, V^{ext} , describing external (mainly large-scale magnetospheric) sources and their Earth-induced counterparts. Both parts are expanded in terms of spherical harmonics.

For the internal part this takes the form

$$V^{\text{int}} = a \sum_{n=1}^{N_{\text{int}}} \sum_{m=0}^n (g_n^m \cos m\phi + h_n^m \sin m\phi) \left(\frac{a}{r}\right)^{n+1} P_n^m(\cos\theta) \quad (1)$$

where $a = 6371.2\text{km}$ is a reference radius, (r, θ, ϕ) are geographic coordinates, P_n^m are the associated Schmidt semi-normalized Legendre functions ([Winch et al., 2005](#)), $\{g_n^m, h_n^m\}$ are the Gauss coefficients describing internal sources, and N_{int} is the maximum degree and order of the internal expansion.

The internal Gauss coefficients $\{g_n^m(t), h_n^m(t)\}, n \leq 20$ are time-dependent, with order 6 B-splines at a 0.5 year knot separation. Higher degree terms, $21 \leq n \leq N_{\text{int}}$, are assumed to be static because they describe the time-independent lithospheric field.

Regarding the field caused by external sources, an expansion of the near magnetospheric sources (e.g. magnetospheric ring current) in the *Solar Magnetic (SM)* coordinate system (up to $n = 2$, with special treatment of the $n = 1$ terms) and of remote magnetospheric sources (e.g., magnetotail and magnetopause currents) in *Geocentric Solar Magnetospheric (GSM)* coordinates (also up to $n = 2$, but restricted to order $m = 0$) is as follows:

$$V^{\text{ext}} = a \sum_{n=1}^2 \sum_{m=0}^n (q_n^m \cos mT_d + s_n^m \sin mT_d) \left(\frac{r}{a}\right)^n P_n^m(\cos\theta_d) + a \sum_{n=1}^2 q_n^{0,\text{GSM}} R_n^0(r, \theta, \phi) \quad (2)$$

where θ_d and T_d are dipole co-latitude and dipole local time, respectively. The degree-1 coefficients in SM coordinates depend explicitly on time and are further expanded as

$$q_1^0(t) = \hat{q}_1^0 \left[\varepsilon(t) + \iota(t) \left(\frac{a}{r} \right)^3 \right] + \Delta q_1^0(t) \quad (3a)$$

$$q_1^1(t) = \hat{q}_1^1 \left[\varepsilon(t) + \iota(t) \left(\frac{a}{r} \right)^3 \right] + \Delta q_1^1(t) \quad (3b)$$

$$s_1^1(t) = \hat{s}_1^1 \left[\varepsilon(t) + \iota(t) \left(\frac{a}{r} \right)^3 \right] + \Delta s_1^1(t) \quad (3c)$$

where the terms in brackets describe the magnetic field contribution caused by the magnetospheric ringcurrent and its Earth-induced counterpart as given by the RC index (see Olsen et al. (2014)), $RC(t) = \varepsilon(t) + \iota(t)$, describing the strength of the magnetospheric ring-current.

If RC provided a perfect description of the magnetospheric field at satellite altitude, then the values of the regression coefficients would be $\hat{q}_1^0 = -1$, $\hat{q}_1^1 = \hat{s}_1^1 = 0$ with vanishing "RC baseline corrections" Δq_1^0 , Δq_1^1 and Δs_1^1 . Deviations from these values are permitted via the co-estimated regression factors $\hat{q}_1^0, \hat{q}_1^1, \hat{s}_1^1$ and the non-zero baseline corrections that are solved for, typically in bins of 5 days for Δq_1^0 and 30 days for Δq_1^1 and Δs_1^1 .

In addition to the spherical harmonic coefficients, regression factors and baseline corrections, Euler angles for the rotation between the coordinate systems of the Vector Fluxgate Magnetometer (VFM) and of the Star Imager on each satellite are co-estimated. Because a rotation does not change the length of a vector, magnetic field intensity is not affected by this rotation, which means that only vector data are influenced by the Euler angles.

In addition to the above models of the geomagnetic field produced by large-scale internal and magnetospheric source, CHAOS-X also includes an estimate of the daily variation caused by ionospheric solar-quiet (Sq) currents. This is based on a spherical harmonic expansion, in Quasi-Dipole (QD) coordinates (Richmond, 1995), of harmonics of the daily variation (Sabaka et al., 2002; Sabaka et al., 2004). Day-to-day and seasonal variations in the amplitude of the system, are parameterized via the observed daily values of the solar radio flux at 10.7 cm (2800 MHz) as recorded at the Penticton radio observatory in Canada.

Methodology for Calculating Uncertainty Values

General Approach

We now present the results of tests of our CHAOS-X model against observatory minute mean data, comparing with an industry standard reference model, the BGGM, and then use these results to obtain uncertainty values required for MWD applications. We have essentially conducted two tests; one retrospective analysis with geomagnetic models released after the observatory data, and one predictive analysis, with geomagnetic models released before observatory data. For MWD navigation, the reference models are used in a predictive mode. However, an accurate retrospective model can also be useful for processing aeromagnetic and marine magnetic survey data, and for post processing of magnetic wellbore survey data. Both tests bear similarities to the analysis described by Macmillan and Grindrod (2010).

For the retrospective analysis, we calculate minute-to-minute differences between the observatory data and model predictions over a 10-year period, starting at September 1st 2000 and finishing August 31st 2010. With respect to available satellites, this 10-year period with CHAMP data is similar to the situation today with *Swarm* satellite data now available. *Swarm* is expected to measure Earth's magnetic field for the next 10 years or so. For this particular study, a *pre-Swarm* version of CHAOS-X (based on the CHAOS-4 field model (Olsen et al., 2014), supplemented by the Sq model described above) and BGGM-2013 were used. In the predictive analysis, we calculate minute-to-minute differences between the observatory data and

model predictions over a 6-month period starting September 1st 2015 and finishing February 29th 2016. The CHAOS-X predictions were calculated based on the CHAOS-5 field model available in August 2015 (Finlay et al., 2015), and the BGGM predictions were found using BGGM-2015.

The raw minute-to-minute differences between observatory data and model predictions are dominated by static biases. These biases are crustal anomalies caused by the small length-scale lithospheric field not included in geomagnetic reference models. These are typically much larger at observatories than at offshore drilling locations. Following Macmillan and Grindrod (2010) we therefore first remove an estimate of the crustal bias for each time series, and calculate the remaining error. The final uncertainty values are then obtained by combining these values with an error estimate for the crustal bias at a typical drilling location.

Geomagnetic Observatory Data

The locations of the observatories used in this work, are shown in Fig. 2. In the retrospective analysis, 108 ground magnetic observatories were used, whereas 59 observatories were used in the predictive analysis. There are less observatories included in the predictive analysis since validated data were not available for many observatories in the actual time period. The locations span all latitudes, but are more numerous at mid-latitudes in the Northern hemisphere, particularly in Europe and North America.

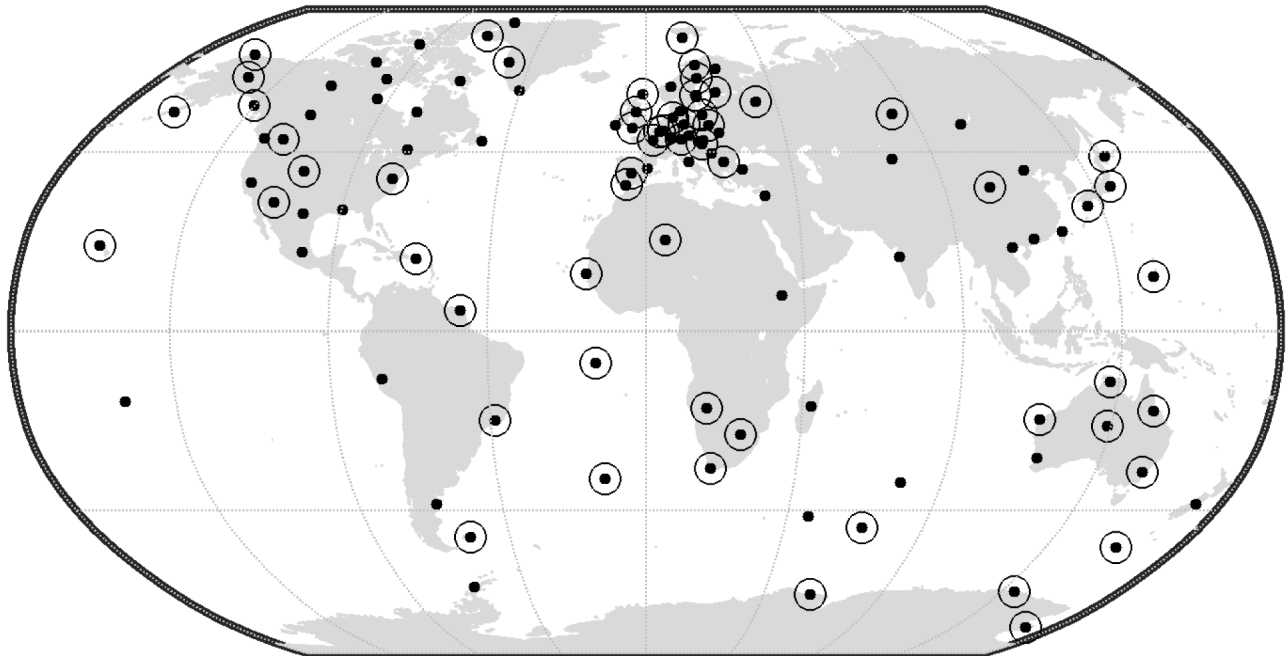


Figure 2—Locations of ground magnetic observatories used in the analyses in this paper. Filled circles indicate the 108 observatories used in the retrospective analysis. Additional larger open circles are added to the 59 observatories used in the predictive analysis.

Estimating Errors for Geomagnetic Reference Models

To obtain error estimates for geomagnetic reference models, we compute the differences ΔG between observatory measurements G_{obs} and model predictions $G_{\text{mod, corr}}$ at a particular location and time, i.e.,

$$\Delta G = G_{\text{obs}} - G_{\text{mod, corr}}, \quad (4)$$

where G is any of the magnetic field elements (declination D , dip angle I or total field intensity F). As the subscript suggests, the model predictions $G_{\text{mod, corr}}$ in Eq. (4) have been corrected for crustal bias by adding estimates of the crustal bias to the model predictions in orthogonal vector components (XYZ corresponding to the north, east and vertical downward components) before transforming to DIF coordinates. Next, difference distributions are investigated individually for each observatory, as a function of geomagnetic latitude and

globally. An example of modelled and observed time series, after the removal of the crustal bias (see below) is shown in Fig. 3.

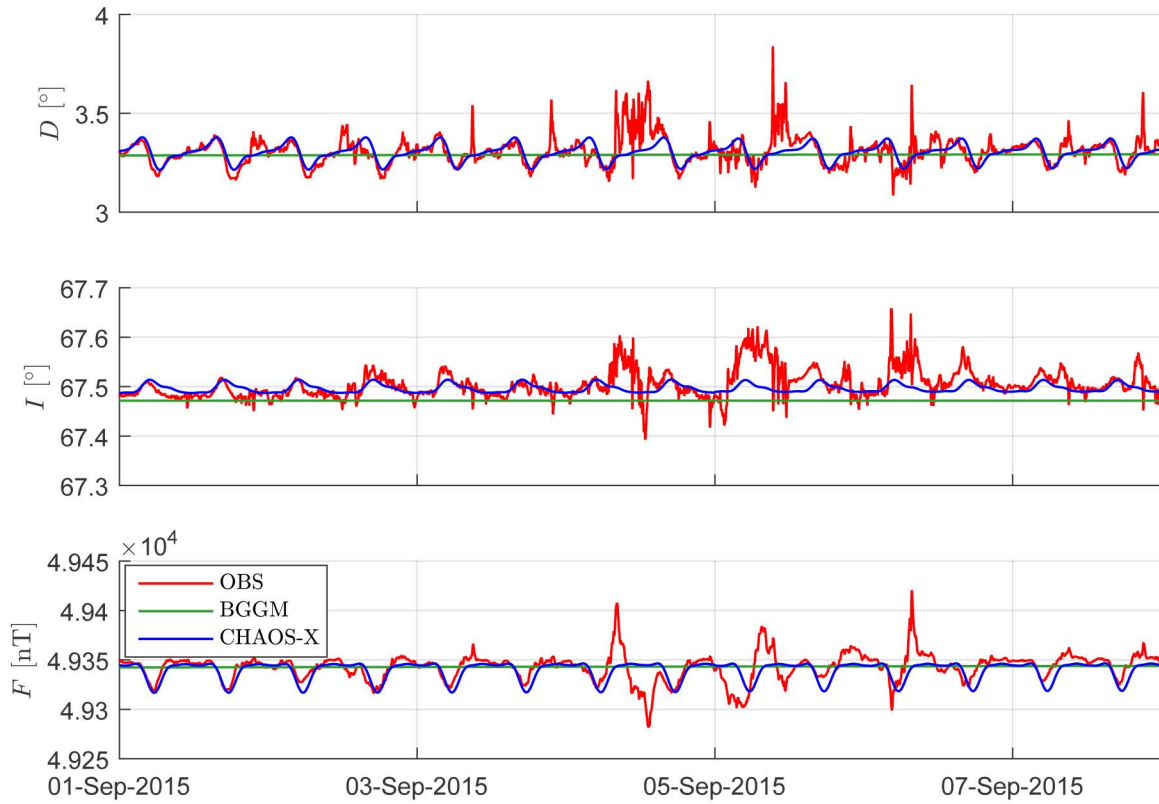


Figure 3—Example from the Niemegek (NGK) observatory, Germany, of a comparison between D , I , F minute mean observational data and model predictions.

The crustal biases were determined for each reference model at each observatory location as follows:

$$\mathbf{B}_{cb} = \overline{\mathbf{B}_{qHVMV}} - \mathbf{B}_{Sq} - \mathbf{B}_{ext} - \mathbf{B}_{int}. \quad (5)$$

where the overbar denotes the (robustly estimated) mean value over all input times, \mathbf{B}_{qHVMV} represents the three vector components (XYZ) of hourly mean observational data values, selected for quiet geomagnetic conditions (such that the change of the D_{st} -index (Sugiura, 1964) must not exceed 2nT/h, and the Kp -index (Bartels et al., 1939; Menvielle and Berthelier, 1991; GFZ, 2016) must fulfill $Kp \leq 2o$), \mathbf{B}_{Sq} are the vector field values predicted at these times by our Sq model, \mathbf{B}_{ext} are predictions for the large scale magnetospheric sources, and \mathbf{B}_{int} are the magnetic field predictions for the internal sources (core and crust) included for each considered model. The crustal biases obtained by this procedure, are consistent with those determined in previous studies (Mandea and Langlais, 2002; Sabaka et al., 2002).

In regions with a small horizontal component of the geomagnetic field B_H , the errors in the declination are 1 to 2 orders of magnitude larger than in other regions. Hence, we find it appropriate to scale the declination error with B_H in figures showing the declination error as a function of QD latitude. For this, and also for finding appropriate values of the AZ and DBH terms of the declination error, we calculate one representative value of B_H for each observatory by averaging the observatory minute mean data over the studied time interval.

In general, we find that the distributions of errors after the removal of the crustal bias fields are non-Gaussian, non-symmetric and do not have zero mean. Furthermore, the typical shape of these distributions varies from observatory to observatory and differs for D , I and F . Therefore, in what follows, we do not

assume any specific underlying probability distribution. Instead, we find it useful to find confidence limits C_{lim} such that

$$P(|\Delta G| \leq C_{\text{lim}}) = p, \quad (6)$$

where $P(|\Delta G| \leq C_{\text{lim}})$ is the cumulative distribution function obtained when taking the absolute value of the differences and p is the associated confidence level. A simpler measure of the difference distribution is the root-mean-squared difference ΔG_{rms} , calculated by

$$\Delta G_{\text{rms}} = \sqrt{\frac{1}{N} \sum_{i=1}^N (\Delta G_i)^2}, \quad (7)$$

where N is the number of differences included in the distribution. We also provide results for the mean differences

$$\overline{\Delta G} = \frac{1}{N} \sum_{i=1}^N \Delta G_i. \quad (8)$$

Results

Time Series Example

Compared with the BGGM model, CHAOS-X in particular has a more detailed description of the external sources. The time series in Fig. 3 show that CHAOS-X yields a more accurate description of the rapid variations in the geomagnetic field. For the example in Fig. 3, the models are used in predictive mode. Compared with the example in Fig. 1, where the models are used in retrospective mode, it is clear that irregular rapid variations in the geomagnetic field are not followed closely, when used in predictive mode.

Retrospective Analysis

The ISCWSA error values have traditionally been estimated based on a regional analysis in the North Sea area (Williamson, 2000; Macmillan and Grindrod, 2010). To this end, we also first perform a North Sea analysis including the five observatories at Lerwick (LER), Eskdalemuir (ESK), Dombås (DOB), Brorfelde (BFE) and Wingst (WNG). The resulting difference distributions are given in Fig. 4 and the resulting error values are given in Table 2.

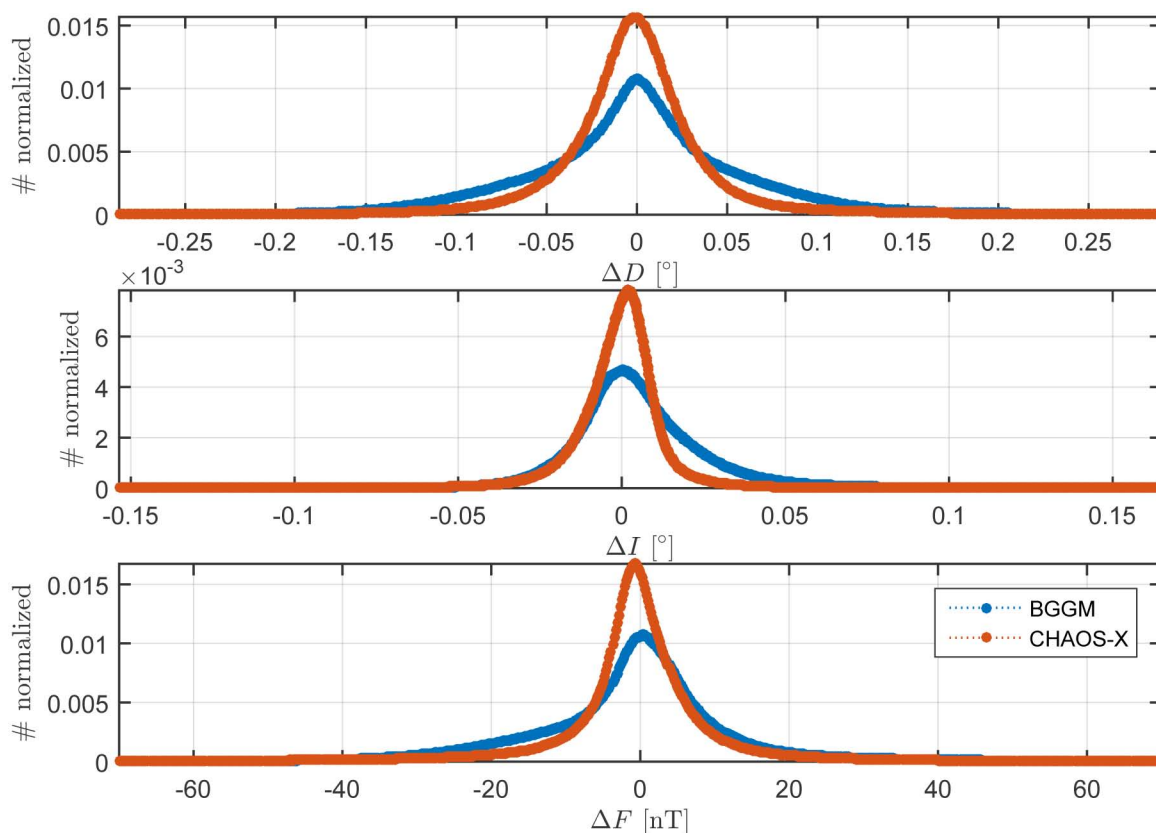


Figure 4—Histogram of the differences ΔD , ΔI and ΔF for 5 observatories in proximity of the North Sea.

Table 2—Confidence levels of differences between observatory data corrected for crustal bias and CHAOS-X and BGGM models. Differences for the regional data set of 5 North Sea observatories are included.

	ΔD [°]		ΔI [°]		ΔF [nT]	
	CHAOS-X	BGGM	CHAOS-X	BGGM	CHAOS-X	BGGM
$C_{lim}(p = 0.683)$	0.030	0.054	0.010	0.017	6.8	10.9
$C_{lim}(p = 0.900)$	0.066	0.103	0.021	0.033	20.8	25.8
$C_{lim}(p = 0.950)$	0.097	0.132	0.030	0.045	37.6	38.8
$C_{lim}(p = 0.954)$	0.101	0.135	0.031	0.047	40.2	41.0
$C_{lim}(p = 0.990)$	0.205	0.226	0.067	0.090	112.6	110.3
$C_{lim}(p = 0.997)$	0.326	0.355	0.151	0.174	200.7	196.4
ΔG_{rms}	0.056	0.072	0.027	0.032	26.3	26.9
$\overline{\Delta G}$	-0.0001	0.0018	-0.0006	0.0056	-1.8070	-1.9895

The results show that CHAOS-X yields smaller errors than BGGM for all elements and confidence levels, except for the two highest confidence levels in the total field intensity value (where our error estimates are only 2 % larger). CHAOS-X performs significantly better than BGGM at lower confidence levels, whereas the models are more similar at higher confidence levels. Lower confidence levels typically correspond to geomagnetically quiet times when field variations are dominated by regular magnetospheric currents and the Sq current system, which are included in CHAOS-X. High confidence levels typically correspond to geomagnetically disturbed times. At such times the fluctuations of the geomagnetic field in the North Sea

region are influenced by the polar electrojet and field aligned current systems, which are strong and difficult to model for both the BGGM and CHAOS-X models.

The confidence limits for the differences when comparing the two models globally are given in Table 3. Qualitatively, the same trend can be seen here, as for the North Sea regional data set discussed above. Namely, that for lower confidence levels, CHAOS-X performs better than BGGM, whereas they perform similarly at high confidence levels.

Table 3—Confidence levels of differences between observatory data corrected for crustal bias and CHAOS-X and BGGM models. Differences for the global set of 108 observatories are included.

	ΔD		ΔI		ΔF	
	[°]		[°]		[nT]	
	CHAOS-X	BGGM	CHAOS-X	BGGM	CHAOS-X	BGGM
$C_{lim}(p = 0.683)$	0.028	0.047	0.011	0.019	7.7	12.8
$C_{lim}(p = 0.900)$	0.096	0.130	0.028	0.046	23.8	34.3
$C_{lim}(p = 0.950)$	0.232	0.287	0.048	0.070	45.7	57.5
$C_{lim}(p = 0.954)$	0.257	0.319	0.052	0.074	49.2	61.0
$C_{lim}(p = 0.990)$	1.111	1.364	0.155	0.173	137.1	146.1
$C_{lim}(p = 0.997)$	2.426	2.884	0.292	0.308	226.4	234.1
ΔG_{rms}	0.306	0.355	0.038	0.044	30.1	33.6
$\overline{\Delta G}$	0.0032	-0.0001	0.0011	0.0022	-0.5717	-1.3332

The magnitude of the differences between model predictions and ground observatory observations vary significantly with location. It is thus important to point out that differences obtained at two different locations typically will contribute to different parts of the global distributions. For instance, the tails of the difference distributions will mainly consist of data obtained at high-latitude observatories where geomagnetic disturbance levels are high. Consequently, global error values based on high confidence levels will be related to the model performance at high latitude or during disturbed times. Such effects must be kept in mind when the results of this Section are evaluated, and care should be taken when global error values are interpreted for a specific location.

In Figs. 5, 6 and 7, results for the root-mean-squared differences as a function of QD magnetic latitude (Richmond, 1995) are presented. It is convenient to study geomagnetic model errors in this coordinate system, because many of the unmodelled disturbance effects to some extent are organized in magnetic latitude. The results show that error values typically are small at low- and mid-latitudes and larger at high QD latitudes. For the total field intensity F , there is a characteristic bump with increased error values at equatorial latitudes. At these latitudes, the unmodelled fluctuations of both the ionospheric Sq variations and the magnetospheric ring current are visible in F . When comparing the two models, the results show that CHAOS-X yields significantly smaller errors, particularly at low- and mid-latitude observatories. This is consistent with CHAOS-X describing magnetospheric currents and the Sq current system more accurately. For example, the BGGM error distribution possesses peak near ± 20 degrees QD latitude in the magnetic dip I that are not present for CHAOS-X, probably because it better models the low-latitude Sq current system including the equatorial electrojet. At higher QD latitudes the two models have similar errors. These regions are dominated by unmodelled polar ionospheric currents.

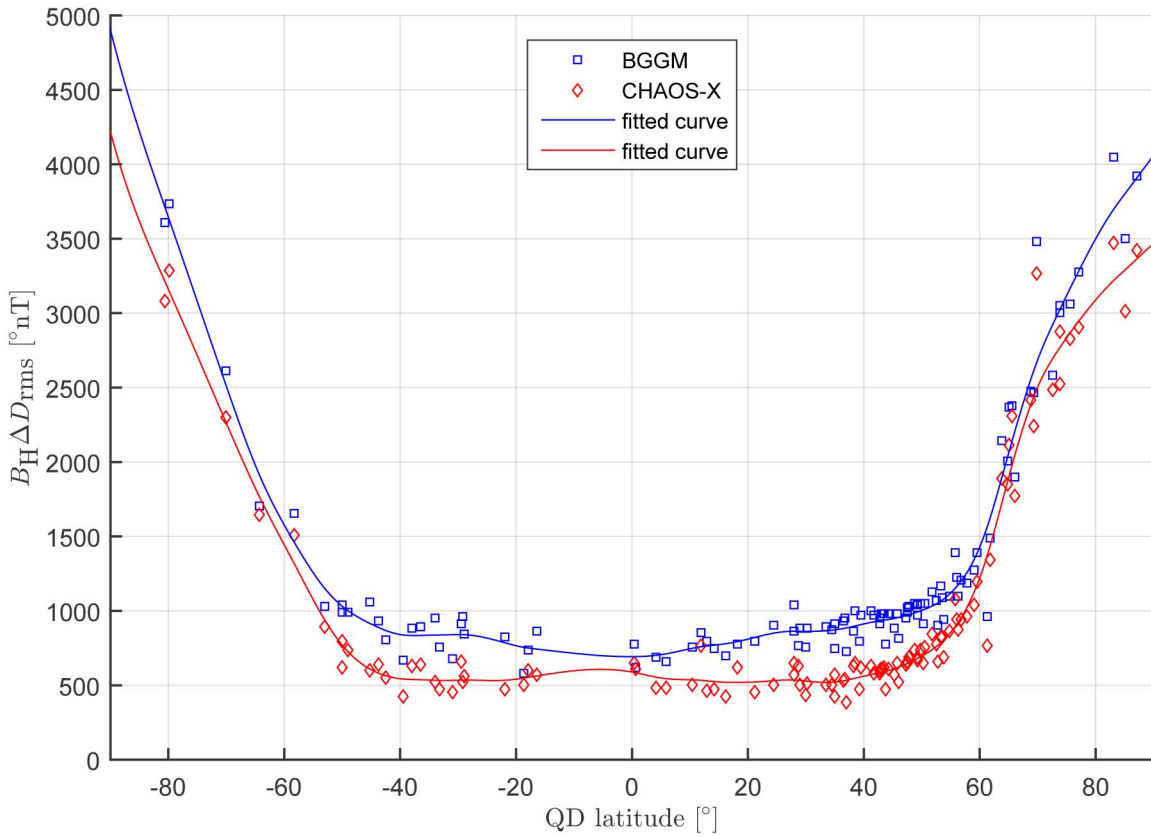


Figure 5—Root-mean-squared difference of the declination D scaled with B_H , as a function of QD latitude. The figure shows results for the two considered models. The solid curves are smoothing spline fits to the data points for each model. Observatory data have been corrected for crustal bias.

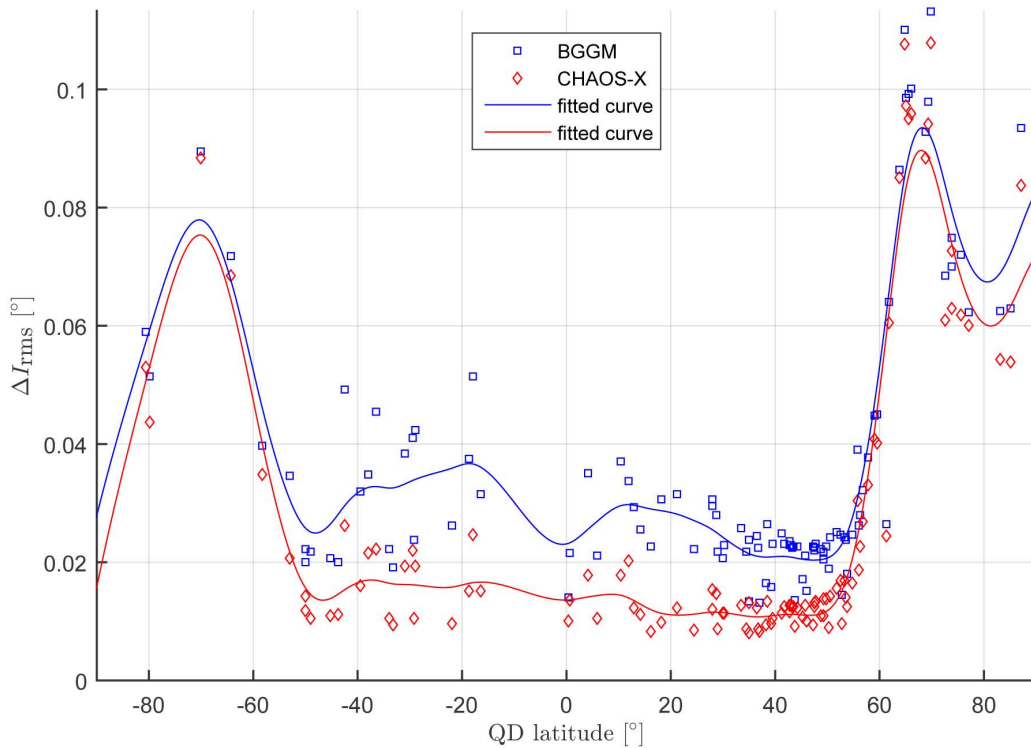


Figure 6—Root-mean-squared difference of the magnetic dip angle I as a function of QD latitude. The figure shows results for the two considered models. The solid curves are smoothing spline fits to the data points for each model. Observatory data is corrected for crustal bias.

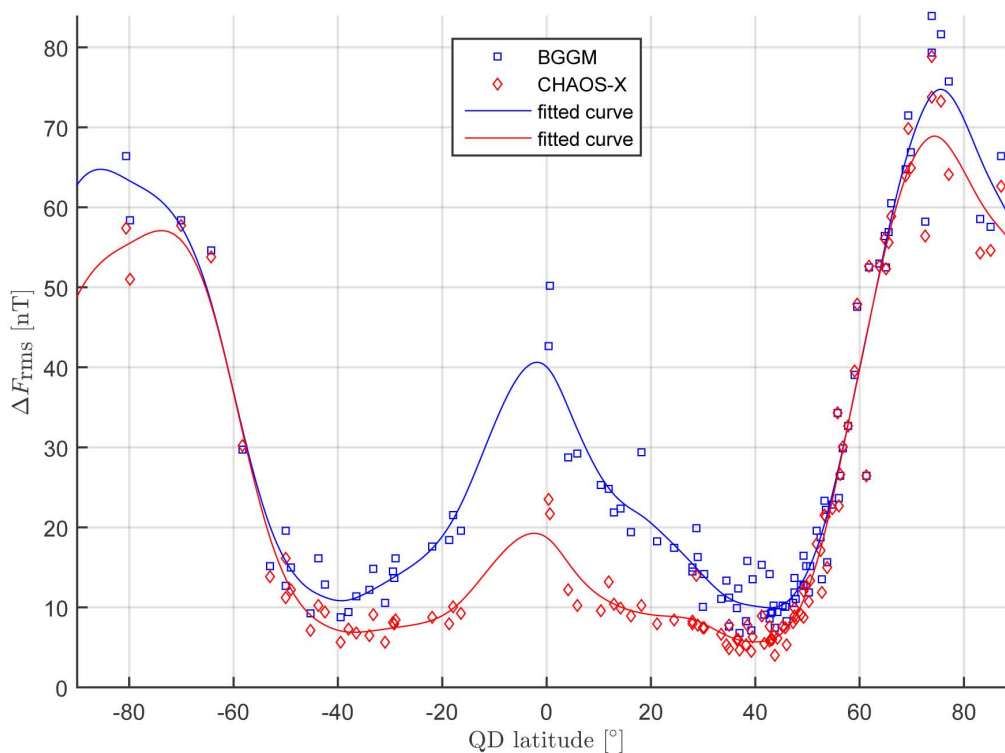


Figure 7—Root-mean-squared difference of the total magnetic field F as a function of QD latitude. The figure shows results for the two considered models. The solid curves are smoothing spline fits to the data points for each model. Observatory data is corrected for crustal bias.

Predictive Analysis

For real-time MWD navigation, the industry uses reference models in a predictive mode. That is, for the comparison between the magnetic field measurements and the reference model, that is needed to find the orientation of the BHA, the reference model is published *prior* to the measurements. This introduces additional errors associated with temporal variation of the geomagnetic field between publication and measurement, and to minimize this error, reference models are updated frequently.

In the predictive analysis, the RC and $F10.7$ indices used for calculating external field variations are estimated in a predictive manner. For each 30-day period, the RC and $F10.7$ indices were estimated as the mean value of index values from the previous 60-day period (30-day period for $F10.7$). It should be mentioned that this is a conservative approach. In future work we plan to develop improved near realtime indices which can be used to improve model predictions at survey stations while drilling. This will improve estimates of previous BHA orientations and current wellbore position.

The results of the predictive analysis are given in Table 4. In addition, for better comparison of the retrospective and predictive analysis, in Figure 8 we plot relative error values, with respect to predictive use of BGGM, for both the retrospective and predictive analysis. Compared with the retrospective analysis, the results show that CHAOS-X errors increases slightly. This is caused by increased errors associated with secular variation of the core field and with using indices in a predictive manner. For the BGGM model, the errors also increase when compared with the retrospective analysis, but the relative increase is less compared with CHAOS-X. This is to be expected since BGGM does not include a detailed external field model and hence does not rely on the geomagnetic indices. Nevertheless, the results of this test clearly show that the performance of CHAOS-X is significantly better than BGGM for low confidence levels when the models are used in a predictive mode.

Table 4—Confidence levels of differences between observatory data corrected for crustal bias and CHAOS-X and BGGM models. In this analysis, the reference models were published prior to the time period, and for CHAOS-X the RC and F10.7 indices are calculated in a predictive manner. A total of 59 observatories are used in this analysis.

	ΔD		ΔI		ΔF	
	[°]		[°]		[nT]	
	CHAOS-X	BGGM	CHAOS-X	BGGM	CHAOS-X	BGGM
$C_{lim}(p = 0.683)$	0.038	0.051	0.027	0.032	15.2	15.6
$C_{lim}(p = 0.900)$	0.134	0.144	0.056	0.061	35.4	38.0
$C_{lim}(p = 0.950)$	0.253	0.293	0.080	0.087	59.6	62.7
$C_{lim}(p = 0.954)$	0.276	0.319	0.083	0.091	63.2	66.3
$C_{lim}(p = 0.990)$	1.120	1.297	0.181	0.193	146.9	152.2
$C_{lim}(p = 0.997)$	2.669	3.128	0.327	0.343	233.5	235.7
ΔG_{rms}	0.319	0.363	0.049	0.053	33.8	34.9
$\overline{\Delta G}$	0.0038	0.0170	0.0046	0.0137	0.2703	-1.838

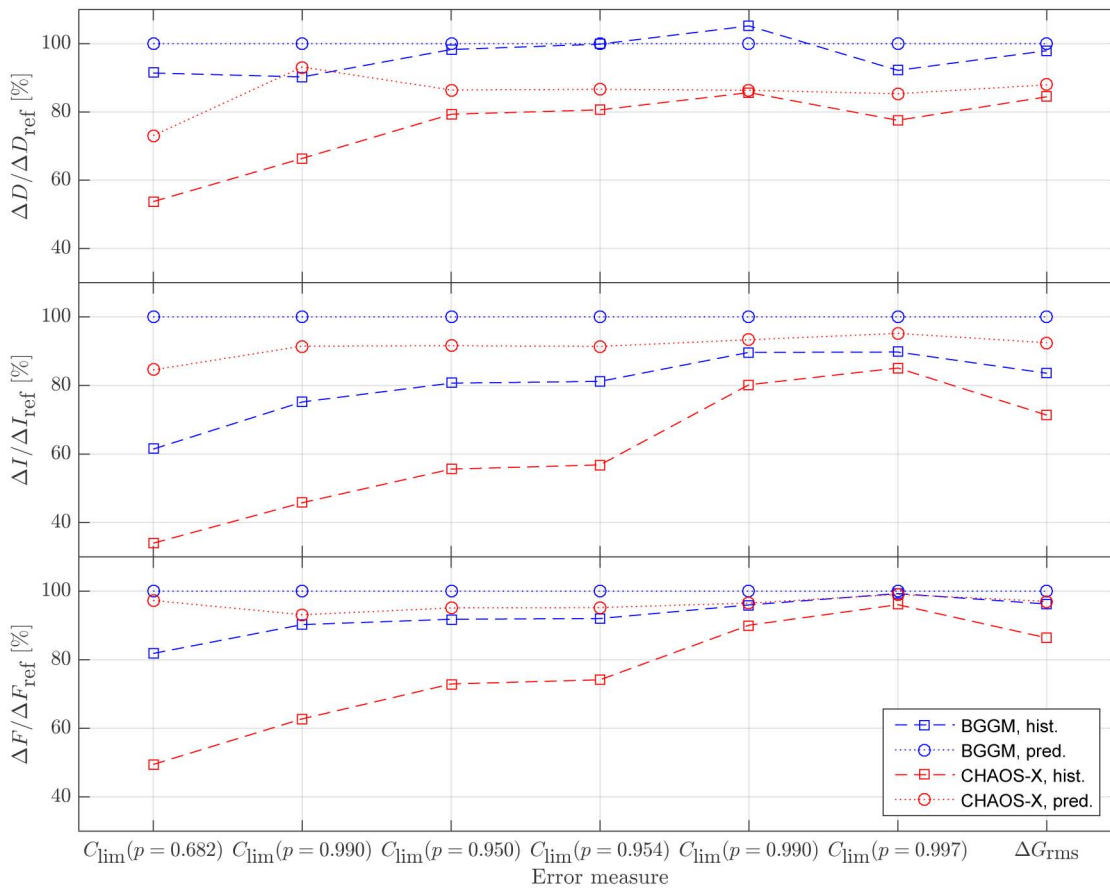


Figure 8—Comparison of relative error for retrospective and predictive analysis. The different error measures are given along the x-axis. The corresponding y-values are the relative error value where ΔG_{ref} , $G \in \{D, I, F\}$ is the error value for BGGM from the predictive analysis. The error values for the retrospective and predictive analysis are taken from Table 3 and Table 4, respectively.

Calculating the ISCWSA Uncertainty Values

As described above, the contributions from the high-degree crustal variations, which are important for the error models used for wellbore accuracy, cannot be deduced in a simple manner from the ground observatory measurements. Macmillan and Grindrod (2010) performed a detailed analysis of the crustal-

field contribution to the BGGM error values, by combining land-based repeat stations and magnetic data in the vicinity of oil and gas fields. Because CHAOS-X is based on similar data and includes approximately the same range of degrees in the spherical harmonic expansion, we expect that the crustal error with our model, in the absence of high resolution information on the local crustal field, will be similar to that associated with the BGGM model. Hence, for calculating error values associated with the ISCWSA error models, we use the same values for crustal errors as published by [Macmillan and Grindrod \(2010\)](#) (see [Table 5](#)), and add these to the error values obtained in the North Sea area ignoring crustal errors, and assuming that the two distributions are independent. We then obtain the results reported in [Table 6](#). In this case, BGGM and CHAOS-X yield similar error values. This is a consequence of the total error being dominated by crustal errors, which are assumed to be equal for the two models in this analysis. To obtain the final ISCWSA values, we used the confidence limit values for $p = 0.954$ to find scaling factors for each element before estimating ISCWSA error values for CHAOS-X by scaling the BGGM values in [Table 1](#). The resulting ISCWSA error values for CHAOS-X are given summarized in [Table 1](#).

Table 5—Values for the BGGM crustal errors, published by [Macmillan and Grindrod \(2010\)](#). The values given here for the root-mean-squared errors are estimated by interpolating data points given by the confidence limits (using Piecewise Cubic Hermite Interpolating Polynomial).

Error Measure	D [°]	I [°]	F [nT]
$C_{lim}(p = 0.683)$	0.167	0.077	80
$C_{lim}(p = 0.900)$	0.411	0.145	144
$C_{lim}(p = 0.950)$	0.679	0.178	169
$C_{lim}(p = 0.954)$	0.719	0.187	171
$C_{lim}(p = 0.990)$	1.416	0.374	245
$C_{lim}(p = 0.997)$	2.153	0.441	320
ΔG_{rms}	0.338	0.098	87

Table 6—Confidence levels of differences between observatory data and CHAOS-X and BGGM models for the North Sea area. Both crustal and temporal errors are included.

Error Measure	ΔD [°]		ΔI [°]		ΔF [nT]	
	CHAOS-X	BGGM	CHAOS-X	BGGM	CHAOS-X	BGGM
$C_{lim}(p = 0.683)$	0.169	0.175	0.078	0.079	80	81
$C_{lim}(p = 0.900)$	0.416	0.423	0.146	0.148	145	146
$C_{lim}(p = 0.950)$	0.685	0.691	0.180	0.183	173	173
$C_{lim}(p = 0.954)$	0.726	0.731	0.189	0.192	175	175
$C_{lim}(p = 0.990)$	1.430	1.433	0.379	0.383	267	267
$C_{lim}(p = 0.997)$	2.176	2.180	0.462	0.469	374	372
ΔG_{rms}	0.342	0.345	0.101	0.103	90	90

Discussion and Conclusion

Comparing the estimated ISCWSA error values in [Table 1](#), CHAOS-X shows only a small improvement compared with the BGGM model. However, this is a consequence of the rather simple manner in which ISCWSA error values are calculated. The values of [Table 1](#) are dominated by errors caused by the small scale crustal field that is assumed unknown. In practice, the small scale crustal field can often be estimated by a separate model based on local magnetic field measurements. In such cases, the crustal errors can be significantly reduced. Then the analysis performed above, shows that CHAOS-X will yield a significant

improvement at low- and mid-latitudes compared with BGGM. We attribute this to a more accurate description of geomagnetic disturbances produced by regular magnetospheric and ionospheric currents. Since these disturbances vary rapidly with time, note that an accurate time stamp must be available to take full advantage of CHAOS-X. At high latitudes, there are large geomagnetic fluctuations produced by ionospheric polar electrojet and field aligned currents, and these are not included in any of the geomagnetic models that are used for MWD purposes. Hence, the errors for all available models are on a similar level at these latitudes. Improved modelling of the auroral electrojet should be of high priority for reducing MWD uncertainties in these regions.

In addition to including crustal errors, the ISCWSA error values are for convenience presented as global error values to be used at any location. This is the case even though they are, for historical reasons, biased towards the North Sea area. However, the accuracy of the geomagnetic models are strongly dependent on location. We agree with [Macmillan and Grindrod \(2010\)](#), that using the coordinates of the actual drilling location when determining the error values associated with the geomagnetic reference model, will produce more realistic uncertainty values associated with the wellbore positioning. Accurate error values for CHAOS-X depending on geographic location can easily be derived on the basis of the analysis in this work.

In this article, we have focused on comparing CHAOS-X with BGGM which is regarded as the industry standard. However, the recently developed HDGM model and successors produced by Magnetic Variation Services LLC, result in smaller ISCWSA error values compared with BGGM. The main reason for this is that such models include a more detailed description of the crustal variations. However, full advantage of including (global or regional) crustal field models can only be taken if external field variations (which are of the same magnitude as the crustal field) are considered. Therefore, in cases where the local crustal field is well known, CHAOS-X with its more accurate description of temporal external variations, will provide a better description of the geomagnetic field.

Acknowledgements

This work has been funded by The Research Council of Norway through the PETROMAKS research programme. Conoco Phillips and Lundin are acknowledged for support through the Northern Area Programme. We would like to thank the staff of the geomagnetic observatories, British Geological Survey, Tromsø Geophysical Observatory and INTERMAGNET for supplying high-quality observatory data. GFZ German Research Centre for Geosciences is acknowledged for providing $K p$ -index values and data from Wingst, Germany.

References

- Bartels, J., Heck, N. H., and Johnston, H. F. 1939. The three-hour-range index measuring geomagnetic activity. *Terrestrial Magnetism and Atmospheric Electricity* **44** (4): 411-454. <http://dx.doi.org/10.1029/TE044i004p00411>.
- BGS. 2016. BGS Global Geomagnetic Model. http://www.geomag.bgs.ac.uk/data_service/directionaldrilling/bggm.html (accessed 22 January 2017).
- Ekseth, R. 1998. *Uncertainties in Connection with the Determination of Wellbore Positions*. PhD thesis. Norwegian University of Science and Technology, Trondheim, Norway (March 1998).
- Ekseth, R., Torkildsen, T., Brooks, A. G., et al. 2006. The reliability problem related to directional survey data. Presented at IADC/SPE Asia Pacific Drilling Technology Conference and Exhibition, 13-15 November, Bangkok, Thailand. IADC/SPE 103734. <http://dx.doi.org/10.2118/103734-MS>.
- Finlay, C. C., Olsen, N., and Toffner-Clausen, L. 2015. DTU candidate field models for IGRF-12 and the CHAOS-5 geomagnetic field model. *Earth, Planets and Space* **67** (1): 1-17. <http://dx.doi.org/10.1186/s40623-015-0274-3>.
- GFZ. 2016. Indices of Global Geomagnetic Activity. www.gfz-potsdam.de/en/kp-index (accessed 22 January 2017).
- ISCWSA. 2016. The Industry Steering Committee on Wellbore Survey Accuracy. <http://iscwsa.org> (accessed 22 January 2017).
- Jamieson, A. 2016. Introduction to wellbore positioning. *University of the Highlands and Islands*. <https://www.uhi.ac.uk/en/research-enterprise/wellbore-positioning-download> (accessed 22 January 2017).

- Macmillan, S. and Grindrod, S. 2010. Confidence Limits Associated With Values of the Earth's Magnetic Field Used for Directional Drilling. *SPE Drilling & Completion* **25** (2): 230-238. <http://dx.doi.org/10.2118/119851-PA>.
- Mandea, M. and Langlais, B. 2002. Observatory crustal magnetic biases during MAGSAT and Orsted satellite missions. *Geophysical Research Letters* **29** (15): ORS 4-1-ORS 4-4. <http://dx.doi.org/10.1029/2001GL013693>.
- Maus, S., Nair, M. C., Poedjono, B., et al. 2012. High Definition Geomagnetic Models: A New Perspective for Improved Wellbore Positioning. Presented at 2012 IADC/SPE Drilling Conference and Exhibition held in San Diego, California, USA, 6-8 March. IADC/SPE 151436. <http://dx.doi.org/10.2118/151436-MS>.
- Menvielle, M. and Berthelier, A. 1991. The K-derived planetary indices: Description and availability. *Reviews of Geophysics* **29** (3): 415-432. <http://dx.doi.org/10.1029/91RG00994>.
- NOAA. 2016. High Definition Geomagnetic Model. <http://ngdc.noaa.gov/geomag/hdgm.shtml> (accessed 22 January 2017).
- Olsen, N., Liihr, H., Sabaka, T. J., et al. 2006. CHAOS-a model of the Earth's magnetic field derived from CHAMP, Orsted, and SAC-C magnetic satellite data. *Geophysical Journal International* **166** (1): 6775. <http://dx.doi.org/10.1111/j.1365-246X.2006.02959.x>.
- Olsen, N., Mandea, M., Sabaka, T. J., et al. 2009. CHAOS-2-a geomagnetic field model derived from one decade of continuous satellite data. *Geophysical Journal International* **179** (3): 1477-1487. <http://dx.doi.org/10.1111/j.1365-246X.2009.04386.x>.
- Olsen, N., Mandea, M., Sabaka, T. J., et al. 2010. The CHAOS-3 geomagnetic field model and candidates for the 11th generation IGRF. *Earth Planets Space* **62**, 719-727. <http://dx.doi.org/10.5047/eps.2010.07.003>.
- Olsen, N., Liihr, H., Finlay, C. C., et al. 2014. The CHAOS-4 geomagnetic field model. *Geophysical Journal International* **197** (2): 815-827. <http://dx.doi.org/10.1093/gji/ggu033>.
- Richmond, A. 1995. Ionospheric Electrodynamics Using Magnetic Apex Coordinates. *J. Geomag. Geoelect.* **47**, 191-212. <http://dx.doi.org/10.5636/jgg.47.191>.
- Sabaka, T. J., Olsen, N., and Langel, R. A. 2002. A comprehensive model of the quiet-time, near-Earth magnetic field: phase 3. *Geophysical Journal International* **151** (1): 32-68. <http://dx.doi.org/10.1046/j.1365-246X.2002.01774.x>.
- Sabaka, T. J., Olsen, N., and Purucker, M. E. 2004. Extending comprehensive models of the Earth's magnetic field with Orsted and CHAMP data. *Geophysical Journal International* **159** (2): 521-547. <http://dx.doi.org/10.1111/j.1365-246X.2004.02421.x>.
- Sugiura, M. 1964. Hourly values of equatorial Dst for IGY. *Ann. Int. Geophys. Year* **35**, 9-45.
- Williamson, H. S. 2000. Accuracy Prediction for Directional Measurement While Drilling. *SPE Drilling & Completion* **14** (4): 221-233. <http://dx.doi.org/10.2118/67616-PA>.
- Williamson, H. S., Gurden, P. A., Kerridge, D. J., et al. 1998. Application of interpolation in-field referencing to remote offshore locations. Presented at SPE Annual Technical Conference and Exhibition, 27-30 September, New Orleans, Louisiana, 221-233. <http://dx.doi.org/10.2118/49061-MS>.
- Winch, D. E., Ivers, D. J., Turner, J. P. R., et al. 2005. Geomagnetism and Schmidt quasi-normalization. *Geophysical Journal International* **160** (2): 487-504. <http://dx.doi.org/10.1111/j.1365-246X.2004.02472.x>.